PHYSICAL REVIEW B VOLUME 50, NUMBER 2 1 JULY 1994-II

Rapid Communications

Rapid Communications are intended for the accelerated publication of important new results and are therefore given priority treatment both in the editorial office and in production. A Rapid Communication in **Physical Review B** *should be no longer than four printed pages and must be accompanied by an abstract. Page proofs are sent to authors.*

Phonon localization and martensitic transformation in Ni_xAl_{1-x} alloys

Silvia Rubini
Centre Européen de Calcul Atomique e Moléculaire, Université Paris-Sud, F-91405 Orsay Cedex, France

Pietro Ballone
Institut für Festkörperforschung, Forschungszentrum Jülich, D-52425 Jülich, Germany

(Received 16 March 1994)

With the embedded-atom method we determine the normal vibrational modes of Ni_xAl_{1-x}, which displays a martensitic transformation (MT) for $0.61 \leq x \leq 0.66$. In the high-temperature phase the compositional disorder induces several bands of localized phonons that discontinuously delocalize at the MT. The analysis of the phonon eigenvectors allows one to identify the atomic arrangements inducing localization. We show that the modes associated with Ni-rich clusters can be used to monitor incipient lattice instabilities, and identify regions with low barriers for nucleation of the martensite.

Waves' localization is a universal manifestation of disorder[1] that has been intensively investigated for electrons, photons, and phonons in random media. In the present study we discuss phonon localization in Ni_xAl_{1-x} for $0.61 \leq x \leq 0.66$. At equilibrium, these compositions correspond to inhomogeneous systems, segregating the NiAl ($B2$, CsCl-type structure) and Ni_3Al ($L1_2$, Cu_3Au-type structure) ordered intermetallic compounds. By quenching from high temperature, however, these alloys can be prepared in a metastable, homogeneous phase, for which the $B2$ (austenite) to $L1_0$ (CuAu-type) (martensite) transition occurs as a martensitic transformation (MT) at a temperature T_M going from ~ 0 K at $x=0.61$ to 400 K at $x=0.66$.[2] Although crystalline and homogeneous, these alloys present concentration disorder, as implied by their off-stoichiometry composition. The computations described below show that in the high-temperature phase this induces several bands of localized modes that discontinuously delocalize at the MT, with the exception of a narrow band of high-frequency Al modes. The analysis of displacement patterns allows to associate a prominent localized band at 7.5 THz to Ni-enriched clusters. We show that these modes manifest a latent local instability of the lattice and identify favorable regions for the nucleation of the martensitic phase. The picture emerging from our computation has clear similarities with the nucleation mechanism proposed by Clapp for ferroelectrics,[3] and already discussed in the literature for the Ni-Al alloys.[4,5] At variance from what is assumed in this theory, however, our results show that in Ni-Al the frequency of the localized modes does not vanish at the martensitic temperature.

The interest in Ni-Al is motivated by the large number of technological applications of these alloys, characterized by a melting temperature above 1600 K, high-temperature strength and creep resistance, stability with respect to oxidation. As a consequence, Ni-Al alloys have been the subject of detailed experimental investigations on their structure, dynamical and mechanical properties, defects, and surfaces.[6] The experimental information relevant for the present study can be summarized as follows. For the composition considered here, the atomic arrangement is easily described starting from the high-T phase where Ni completely fills one of the two simple cubic sublattices of the CsCl structure and the excess Ni atoms occupy random antisite positions on the predominantly Al sublattice.[7] This ordered arrangement is inherited by the martensite, being the MT diffusionless. The phonon dispersion relations have been measured by inelastic neutron scattering, and display an anomalous branch in the [110] direction.[8] The low-energy dip in this branch (that never goes soft) is a crucial factor for the MT, and its precise position determines the structure of the product phase.[9] Finally, particularly relevant is a very recent paper by Shapiro and co-workers,[5] analyzing the behavior of this anomaly in premartensitic $Ni_{0.625}Al_{0.375}$ under uniaxial stress. The connection between their measurements and our results is discussed in the conclusions.

We study the vibrational properties of Ni_xAl_{1-x} in the framework of the embedded-atom-method (EAM),[10] which, although semiempirical, provides a reliable and globally accurate description of these alloys. The details of the potential and the results from an extensive set of tests of its reliability are reported in Ref. 11. Here we remind the following points. Our potential is constructed in order to reproduce the lattice parameter, cohesive energy, bulk modulus, and zone boundary phonons of the pure Ni and Al solids, as well as the excess enthalpy of mixing for the intermetallic NiAl and Ni_3Al. For the intermediate compositions it provides good

vibrational densities of states and elastic constants. It faithfully reproduces the MT, including the high sensitivity of T_M on composition, and its behavior under uniaxial stress.

The configurational disorder is taken into account by performing the computation for supercells containing $N=1024$ atoms. To check the scaling of localization with size, computations for $N=432$ and $N=1296$ are also performed. Following the experimental evidence, we randomly distribute the excess Ni atoms on the Al sublattice. Although the size of the system is sufficiently large to provide a representative model for the extended solid, we average our results over four initial atomic distributions.

Temperature is taken into account by choosing the system volume (both for the CsCl and $L1$ phase) according to the quasiharmonic equation of state computed in Ref. 11. For each composition, configuration, and temperature (i.e., volume) the atomic positions are accurately relaxed to the potential energy minimum by a combination of molecular dynamics and quenches. Then, we compute eigenvalues and eigenvectors for the normal vibrational modes by diagonalizing the dynamical matrix. All the computations have been performed at the Γ point of the Brillouin zone. The model vibrational density of states compares favorably with the experimental one for the compositions and structures for which this information is available.

The analysis of the eigenvectors shows that in the composition range $0.61<x<0.66$, for both the austenitic and the martensitic phases, the vibrational spectrum is divided into two contiguous but almost nonoverlapping regions: a low-frequency domain (up to 7.5 THz) for the modes of Ni, and a high-frequency region (7.5 – 11 THz) for the light Al atoms.

We discuss localization in terms of the inverse participation ratio:[12]

$$p^{-1}=N\frac{\sum_{i=1}^{N}|\vec{B}_i^{\alpha}(\omega_\alpha)|^4}{\left(\sum_{i=1}^{N}|\vec{B}_i^{\alpha}(\omega_\alpha)|^2\right)^2}, \qquad (1)$$

where α labels the normal modes, i the atoms, and the $\vec{B}_i^{\alpha}(\omega_\alpha)$ are the mass-dependent, normalized eigenvectors of the dynamical matrix. A delocalized mode is characterized by $p^{-1}\sim 1$, while localization is indicated by peaks in p^{-1}.

The results for p^{-1} of $Ni_{0.63}Al_{0.37}$ in the CsCl structure at $T=470$ K, i.e., 200 K above the MT, are displayed in Fig. 1(a). Three peaks are apparent in p^{-1}: at 5.8 THz, at 7.4 THz, and at 11 THz. Although not visible on the scale of the main figure, an additional small peak is present at ~ 1.6 THz (see inset). We verified that changing the system size does not modify the position of the peaks, while their amplitude scales linearly with size.

Decreasing the temperature down to T_M changes only slightly the picture above [see Fig. 1(b)]. A discontinuous change, instead, occurs across the transition [see Fig. 1(c)]: the localization peaks disappear at T_M in the martensitic phase, with the exception of the high-frequency band at 11 THz.

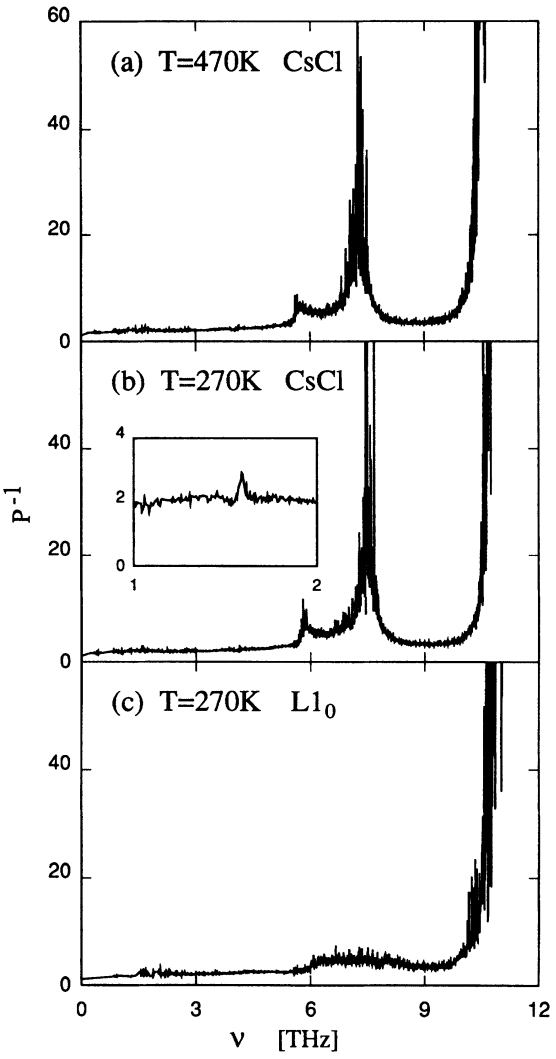

FIG. 1. Inverse participation ratio in $Ni_{0.63}Al_{0.37}$ at high temperature in the CsCl structure (a), and at T_M in the CsCl (b) and $L1$ (c) structures. In the inset in (b) p^{-1} is plotted in an expanded scale in the 1–2 THz range.

Before discussing the relation of localization and MT, we characterize the atomic configurations associated with the localized modes. To this aim, we analyzed the atomic displacements $\vec{u}_i^{\alpha}=\vec{B}_i^{\alpha}/\sqrt{M_i}$ (M_i is the mass of the atom i) for the modes whose p^{-1} exceeds 10. By definition, few atoms display an appreciable displacement for these phonons. For each of the localized modes we select the two atoms with the largest displacement. For convenience, we shall refer to these atoms supporting the localized modes as the "ℓ set." We characterize their local environment by identifying their first- and second-neighbor shells. We distinguish stoichiometric NiAl and Ni_3Al regions, isolated Ni antisites in NiAl regions, and pure Ni clusters. This analysis associates the peak at 5.8 THz with isolated Ni antisites into NiAl regions. The peak at 7.5 THz occurs at the junction of the Ni and Al frequency domains. The Ni modes are associated to Ni-enriched regions (either Ni_3Al or Ni clusters), while the Al modes belong to NiAl regions. The high-frequency localized band at 11 THz corresponds to the Al modes in Ni_3Al re-

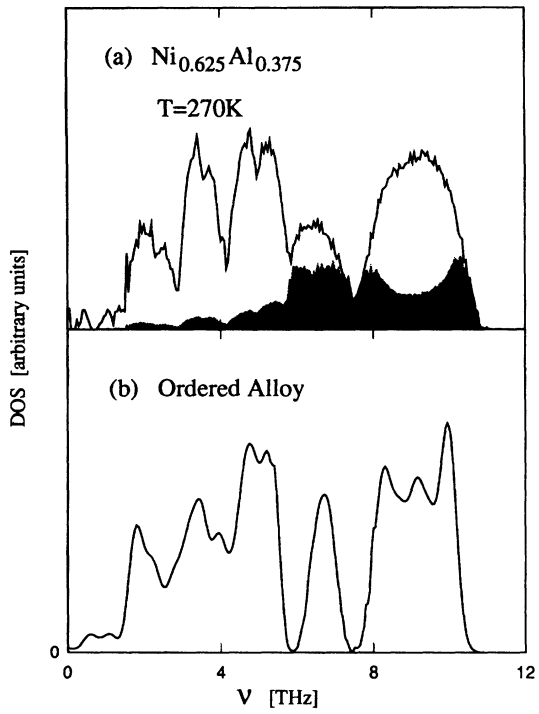

FIG. 2. Vibrational density of states for a disordered (a) and ordered (b) $Ni_{0.63}Al_{0.37}$ alloy. The shaded area in (a) corresponds to the contribution to the DOS arising from the localized modes.

gions. This band, unaltered across T_M, is the simplest to expect and interpret. It corresponds to localized optical modes of a light impurity in a metal, and has several analogs in other systems.[13] In the following, we shall not discuss its behavior, and concentrate on the low- and medium-frequency bands. Finally, the small peak at 1.6 THz corresponds to acoustic modes of pure Ni clusters.

The close relation of localization and composition fluctuations is highlighted by the comparison with an ordered $Ni_{0.625}Al_{0.375}$ structure, prepared (following Fig. 1 of Ref. 14) by regularly replacing with Ni 1/4 of the Al in NiAl. The vibrational density of states (DOS) of this artificial structure is displayed in Fig. 2(b), and compared with that of the alloy with random position of the excess Ni atoms [Fig. 2(a)]. The DOS of these two systems display a clear similarity in the position and amplitude of the peaks, with, however, an important difference. The DOS of the ordered structure presents two gaps at 5.8 THz and 7.5 THz that are partially filled in the alloy with disorder. The modes in the gaps are localized, as apparent by comparison with Fig. 1 and confirmed by the following construction: for each mode we project a "local contribution" $\chi=[1+(p^{-1})^2]/[25+(p^{-1})^2]$ that tends to one as the mode becomes more localized. The DOS associated to this local contribution is represented by the shaded area in Fig. 2(a), from which it is apparent that at 5.8 and 7.5 THz only localized modes are present, and only at these frequencies the contribution of the extended phonons is negligible.

We now turn to the discussion of the relation between localization and the MT. Clearly, the main localized bands are not the driving force behind the MT, since their frequency is too high, and, as shown by their positive Grüneisen parameter $\gamma_i=-\partial \ln\omega_i/\partial \ln V$, they do not present anomalies in approaching the MT. Moreover, the computation of the dynamical structure factor $S(\vec{k},\omega)$ shows that in the [110] direction, usually associated with the transition, the contribution of the localized modes is moderate.

TABLE I. Energy (e_i), stress (σ), and width W_{12} of the shell containing the 12 nearest neighbors for the Ni atoms in $Ni_{0.63}Al_{0.37}$. First row: average over the Ni atoms supporting localized modes (ℓ set). Second row: global average over the Ni atoms in the entire system.

	e_i (eV/atom)	σ^i (kbar)	W_{12} (Å)
ℓ set	−5.32	−79.5	2.04
All Ni atoms	−6.01	14.1	2.31

Despite these observations, the close relation of localization and MT is apparent in the drastic effects of the latter on the former, displayed in Fig. 1. A microscopic analysis of potential energy, stress, and local structure shows that, indeed, the atoms supporting the localized modes present in the austenite significant deviations from the average system properties. More precisely, all the analyzed quantities show that local modes characterize strained, high-energy regions, that provide a favorable environment for the nucleation of the martensite. The correspondence of instability and localization is strongest for the band at 7.5 THz, associated with Ni-rich regions.

Starting from the EAM expression for the cohesive energy

$$E_c=\sum_{i=1}^{N} e_i=\sum_{i=1}^{N}\frac{1}{2}\sum_{j\neq i}\Phi(|\vec{R}^i-\vec{R}^j|)+\sum_i F_i$$

(where Φ is a two-body potential, and F_i is the energy gain in embedding the atom i into the valence electron distribution) we identify e_i with the potential energy of the single atom. In the austenite at T_M, the average of e_i for the atoms in the ℓ set is 0.7 eV higher than the global average. Another indication of incipient local instability comes from the atomic hydrostatic stress $\sigma^{(i)}$, measuring a kind of local pressure, and defined as the trace of $\sigma^{(i)}_{\alpha,\beta}$:[15]

$$\sigma^i_{\alpha,\beta}=\frac{N}{3V}\sum_{j\neq i}\frac{\partial E_c}{\partial(\vec{R}^i_\alpha-\vec{R}^j_\alpha)}(\vec{R}^i_\alpha-\vec{R}^j_\alpha)(\vec{R}^i_\beta-\vec{R}^j_\beta),$$

where V is the system volume, and α, β are Cartesian coordinates. The global average of $\sigma^{(i)}$ is zero, since the system is at zero pressure. The subaverage over the ℓ set, instead, shows that these atoms are highly stretched with respect to their optimal local configuration. For a homogeneous comparison, we report in Table I the average of e_i and σ^i for the Ni atoms with the subaverage restricted to the Ni atoms in the ℓ set. Finally, we analyze the local structure by computing the distances in the first- and second-neighbor shells. At and above T_M, the local structure is bcc-like for all the atoms, with, however, many indications that around the atoms in ℓ there are distortions anticipating the compact martensite. In Table I we report one of the many indices of this distortion, i.e., the width of the shell containing the first 12

neighbors. The average for the atoms in ℓ is significantly narrower than the global average, showing that an fcc coordination is starting to develop around these atoms. Computations at $T<T_M$ show that the deviation of the atoms in ℓ is significantly reduced in the martensitic phase.

Before summarizing our results and discussing the connection with previous papers, we want to point out the peculiarity of the peak at 1.6 THz. For these modes, we compute a negative and large Grüneisen parameter; they contribute to $S(\vec{k},\omega)$ also along [110], and are associated with atoms with high energy, high stress, and significant local distortion. For these reasons, we always considered these modes in our discussion, despite their moderate localization.

In conclusion, we have shown that compositional disorder induces several bands of localized modes in the high-T phase of Ni_xAl_{1-x} $(0.61\leq x\leq 0.66)$. Localization discontinuously disappears across the MT, with the exception of highly localized, optical modes of Al at 11 THz. The analysis of atomic displacements allows us to associate each band to specific local fluctuations in composition. Particularly relevant for our discussion are the modes at 7.5 THz associated with Ni-rich regions. The analysis of local properties shows that these modes characterize regions of high energy, high stress, and local deformation pointing to the compact $L1$ phase, that, therefore, provide favorable nucleation sites for the martensite.

Our observation has a clear relation with the localized soft mode (LSM) picture of Clapp,[3] reproposed in the case of Ni-Al by Zhao and Harmon.[4] This theory has been recently tested by Shapiro and co-workers, with a measure of the phonon dispersion relation along the [110] direction.[5] The effect of the internal stress characterizing regions of composition fluctuation has been simulated by an external stress in the [001] direction. Both the frequency and $\vec{k}$ dependence of the dip in the transverse phonon branch support the predictions of the LSM model.

Our computation provides microscopic evidence for the association of localized modes and incipient local instability of the austenite, and, in this respect, supports the theory by Clapp. Our results, however, highlight also an important difference, since they show that in Ni-Al alloys the frequency of the localized modes does not vanish at the transition. A direct role in the transformation is likely to be played by the modes at 1.6 THz, associated with pure Ni clusters. They are at low frequency, have a negative Grüneisen coefficient close to T_M, and have a relevant weight in the [110] direction of the reciprocal space. The size of our systems prevents a direct investigation of nucleation involving Ni clusters of realistic size. However, it is conceivable that in macroscopic samples of Ni_xAl_{1-x} (whose inhomogeneity is notorious), highly enriched Ni regions occur with sufficient frequency to provide the $\sim 10^6$ nuclei/cm^3 measured in experiments,[16] and that the modes at 1.6 THz correspond indeed to the "nearly soft" modes required by the LSM model.

The localized bands at 5.8 THz and 7.5 THz do not soften going toward the T_M, and their frequency is too high to suggest a direct role in determining the transition. However, also these modes identify unfavored regions in the austenite phase, already presenting local distortions anticipating the martensite. These modes are, in fact, the vibrations of Ni-rich clusters that do not participate in the vibrations of the surrounding solid because of the high stress characterizing the clusters. These regions provide additional and abundant sites for the nucleation of the martensite.

We are grateful to S. de Gironcoli and R. Gotthardt for useful discussions and a careful reading of the manuscript.

[1] P. W. Anderson, Phys. Rev. **109**, 1492 (1958); Rev. Mod. Phys. **50**, 191 (1978).

[2] M. F. Singleton, J. L. Murray, and P. Nash, in *Binary Alloy Phase Diagram*, edited by T. B. Massalski (American Society for Metals, Metal Park, OH, 1986).

[3] P. C. Clapp, Phys. Status Solidi B **57**, 561 (1973); Ferroelectrics **16**, 89 (1977).

[4] G. L. Zhao and B. N. Harmon, Phys. Rev. B **45**, 2818 (1992).

[5] S. M. Shapiro *et al.*, Phys. Rev. B **48**, 13 223 (1993).

[6] D. B. Miracle, Acta Metall. Mater. **41**, 649 (1993).

[7] A. J. Bradley and A. Taylor, Proc. R. Soc. **A159**, 56 (1937).

[8] S. M. Shapiro *et al.*, Phys. Rev. Lett. **62**, 1298 (1988); M. Mostoller *et al.*, Phys. Rev. B **40**, 2856 (1989); S. M. Shapiro *et al.*, *ibid.* **44**, 9301 (1991).

[9] J. Krumhansl and R. J. Gooding, Phys. Rev. B **39**, 3047 (1989).

[10] M. S. Daw and M. I. Baskes, Phys. Rev. B **29**, 6443 (1984).

[11] S. Rubini and P. Ballone, Phys. Rev. B **48**, 99 (1993).

[12] R. J. Bell, P. Dean, and D. C. Hibbins-Butler, J. Phys. C **3**, 2111 (1970); W. M. Visscher, J. Non-Cryst. Solids **8-10**, 477 (1972).

[13] H. Böttger, *Principles of the Theory of Lattice Dynamics* (Physik Verlag, Berlin, 1983).

[14] C. S. Becquart, P. C. Clapp, and J. A. Rifkin, Phys. Rev. B **48**, 6 (1993).

[15] T. Egami and D. Srolovitz, J. Phys. F **12**, 2141 (1982).

[16] R. E. Cech and D. Turnbull, Trans. AIME **206**, 124 (1956).

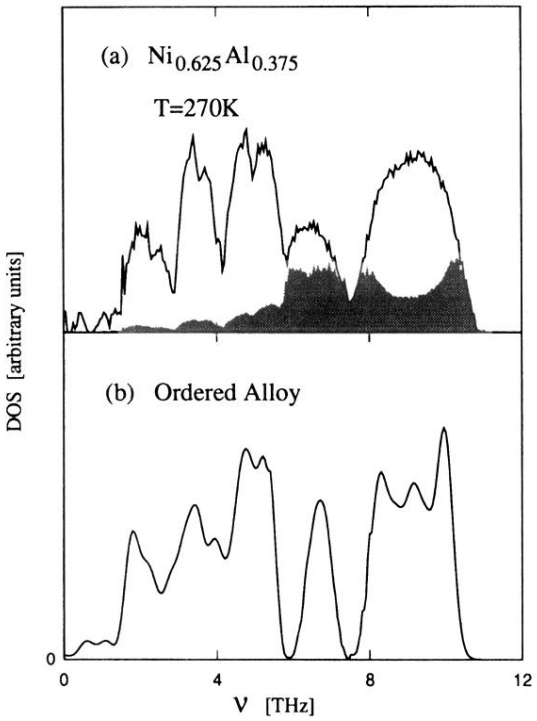

FIG. 2. Vibrational density of states for a disordered (a) and ordered (b) $Ni_{0.63}Al_{0.37}$ alloy. The shaded area in (a) corresponds to the contribution to the DOS arising from the localized modes.